Eur. Phys. J. D **16**, 391–394 (2001)

THE EUROPEAN PHYSICAL JOURNAL D

EDP Sciences

Electronic structures in coupled two quantum dots by 3D-mesh Hartree-Fock-Kohn-Sham calculation

T. Matsuse[a], T. Hama, H. Kaihatsu, N. Toyoda, and T. Takizawa

Faculty of Textile Science and Technology, Shinshu University, Ueda, Nagano 386-8567, Japan

Received 30 November 2000

Abstract. To study the electronic structures of quantum dots in the framework of self-interaction-free including three dimensional effects, we adopt the theory of nonlocal effective potential introduced by Kohn and Sham [1]. For utilizing the advantageous point of the real space (3D) mesh method to solve the original nonlinear and nonlocal Hartree-Fock-Kohn-Sham (HFKS)-equation, we introduce a linearization of the equation in the local form by introducing the local Coulomb potentials which depend on explicitly the two single particle states. In practice, for solving the local form HFKS-equation, we use the Car-Parrinello-like relaxation method and the Coulomb potentials are obtained by solving the Poisson equation under proper boundary conditions. Firstly the observed energy gap between triplet- and singlet-states of $N = 4$ in DBS [7] is discussed to reproduce the addition energies and chemical potentials depending the magnetic field. Next the coupling between two-quantum dots in TBS [8] is studied by adding the square barrier between two dots. The spin-degeneracy [8] measured in gate-voltage depending on magnetic field is well reproduced in the limit of small mismatch. Finally, the electronic states in the ring structure are calculated and discussed how the ring size and magnetic field affect to the structures.

PACS. 73.20.Dx Electron states in low-dimensional structures (superlattices, quantum well structures and multilayers) – 71.15.Fv Atomic- and molecular-orbital methods (including tight binding approximation, valence-bond method, etc.)

1 Introduction

Although Kohn and Sham [1] have pointed out the theory of nonlocal effective potential which introduces the correlation energy functional to the Hartree-Fock energy for calculating the electronic structures of the many electron system from the view point of density functional theory, almost all calculations performed until now by real space mesh method are those of LDA and LSDA which have an inherent problem of self-interaction [2].

In this report we show the straightforward application of the Hartree-Fock-Kohn-Sham (HFKS) theory [3] to the self-interaction free calculation of the electronic structures in many electron system by using 3D-mesh method.

Firstly the method of linearization of the original nonlocal and nonlinear HF-equation in the local form is shown to solve the equation by utilizing the advantageous point of the real space (3D) mesh method which has been developed in the field of nuclear physics [4]. Next we apply this 3D-mesh HFKS-calculation to the study of the electronic structure in the artificial atom and molecule in the vertical quantum dots realized between the heterostructure barriers [7,8].

The presented HFKS-calculation is a kind of unrestricted HFKS-calculation (UHFKS-calculation), because it becomes equivalent to the well-known unrestricted HF calculation of the original Hartree-Fock approximation when we neglect the correlation energy in the HFKS-calculation.

[a] e-mail: matsuse@jolie.shinshu-u.ac.jp

2 Local form of HFKS equation

According to Kohn and Sham [1], the energy functional of N electron system $E_{HFKS} = E_{HF} + E_c[\rho^\alpha, \rho^\beta]$ is composed of Hartree-Fock energy E_{HF} and correlation energy $E_c[\rho^\alpha, \rho^\beta]$. In this report we use the correlation energy of the local spin density functional presented by Vosko and Wilk [5]. After the variation of the HFKS-energy functional, the original HFKS-equation is obtained as follows,

$$[h(\mathbf{r}) + U_H(\mathbf{r})]\psi_i^\sigma(\mathbf{r}) - \sum_{j=1}^{N_\sigma} \int \frac{\psi_j^{\sigma *}(\mathbf{r}')\psi_i^\sigma(\mathbf{r}')}{|\mathbf{r} - \mathbf{r}'|}\psi_j^\sigma(\mathbf{r})d\mathbf{r}' + v_c^\sigma([\rho^\alpha, \rho^\beta], \mathbf{r})\psi_i^\sigma(\mathbf{r}) = \epsilon_i^\sigma \psi_i^\sigma(\mathbf{r}). \quad (1)$$

To linearize this nonlocal and nonlinear equation, the usual nonlocal form is not suitable for the real space mesh method.

However, we can linearize the original HFKS-equation in the local form as is shown in the following equation,

$$[h(\mathbf{r}) + U_H(\mathbf{r})]\psi_i^\sigma(\mathbf{r}) - \sum_{j=1}^{N_\sigma} U_{ij}^\sigma(\mathbf{r})\psi_j^\sigma(\mathbf{r}) + v_c^\sigma([\rho^\alpha, \rho^\beta], \mathbf{r})\psi_i^\sigma(\mathbf{r}) = \epsilon_i^\sigma \psi_i^\sigma(\mathbf{r}) \quad (2)$$

by introducing the Coulomb potentials $U_{ij}^\sigma(\mathbf{r})$ which depends explicitly the single particle states

$$U_{ij}^\sigma(\mathbf{r}) = \int \frac{1}{|\mathbf{r} - \mathbf{r}'|}\rho_{ij}^\sigma(\mathbf{r}')d\mathbf{r}' \quad (3)$$

where $\rho_{ij}^\sigma(\mathbf{r}) = \psi_j^{\sigma *}(\mathbf{r})\psi_i^\sigma(\mathbf{r})$.

Here $h(\mathbf{r})$ denotes a one-body part of the system and $U_H(\mathbf{r})$ the Hartree term. Third term is the exchange potentials and the fourth one $v_c^\sigma([\rho^\alpha, \rho^\beta], \mathbf{r})$ spin-dependent local correlation potential.

In practice, for obtaining the self-consistent solution of the local form HFKS-equation (2), we use the Car-Parrinello-like relaxation method and the Coulomb potentials (3) are calculated by solving the Poisson equation $\nabla_{\mathbf{r}}^2 U_{ij}^\sigma(\mathbf{r}) = -4\pi\rho_{ij}^\sigma(\mathbf{r})$ under the proper boundary conditions. To calculate the kinetic energy in this 3D-mesh calculation, the finite difference is applied by using about 13 mesh points.

3 Electronic structures in single quantum dot

To calculate the electronic structure of a quantum dot of N-electrons including 3-dimensional effect, we use the following the total Hamiltonian for HF-part

$$\hat{H}_N = \sum_{i=1}^{N} \hat{H}_{XY}(x_i, y_i) + \frac{1}{2}\sum_i \sum_{j \atop i \neq j} \frac{e^2}{\epsilon|\mathbf{r}_i - \mathbf{r}_j|} + \sum_{i=1}^{N} \hat{H}_Z(z_i) \quad (4)$$

where $\hat{H}_{XY}(x,y) = -\frac{\hbar^2}{2m^*}\nabla_{xy}^2 + U_C(x,y) + U_B(x,y)$ is the usual 2-dimensional Hamiltonian. The confinement potential $U_C(x,y) = \frac{1}{2}m^*\omega_0^2(x^2+y^2)$ is used and the magnetic field effect is represented by $U_B(x,y) = \frac{1}{2}m^*\frac{\omega_c^2}{4}(x^2+y^2) + \frac{\omega_c}{2}\hat{l}_z + g^*\mu_B\frac{\mathbf{B}\cdot\mathbf{S}}{\hbar}$ where $\omega_c = \frac{eB}{m^*}c$ is cyclotron frequency. In this calculation, we use the effective mass of $m^* = 0.067$ and the effective g-factor $g^* = 0.44$. For the dielectric constant we use a value of $\epsilon = 12.5$ for UHFKS-calculation, but we change the value to $\epsilon = 25.8$ for UHF-calculation as will be discussed below.

The vertical degree of freedom in the quantum dot is introduced in $\hat{H}_Z(z)$ with potential $U_Z(z)$ of square well form; $\hat{H}_Z(z) = -\frac{\hbar^2}{2m^*}\frac{\partial^2}{\partial z^2} + U_Z(z)$. All geometrical factors in $\hat{H}_Z(z)$ are settled to be the almost same scale shown in Refs. [7,8]. For the case of single Q-dot, the length of the z-direction is 12 nm and divided in 11 mesh points.

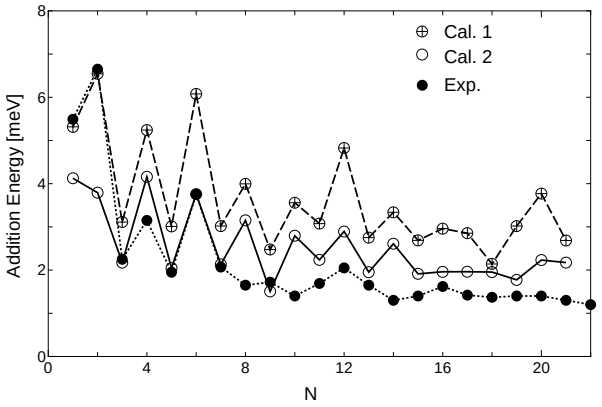

Fig. 1. Electron number dependence of addition energy by 3D-mesh UHFKS calculation and comparison with experimental ones [7]. Cal.1 and Cal.2 are for $\hbar\omega = 5$ meV and 3 meV, respectively.

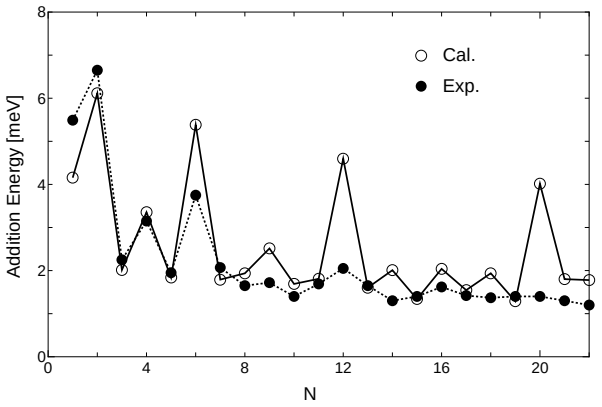

Fig. 2. Electron number dependence of addition energy of 3D-mesh UHF-calculation and comparison with experimental ones [7]. Cal is for $\hbar\omega_0 = 5$ meV and $\epsilon = 25.8$.

The maximum value of the xy-plane is settled as 100 nm and divided in 21 mesh points with equidistance for the case of confinement potential $\hbar\omega = 5$ meV and 130 nm for $\hbar\omega = 3$ meV.

In this single Q-dot, it had been verified that the wave functions in the vertical direction were composed of the ground state wave function with almost sine shape and the function weaken considerably the two-body Coulomb energy of the two dimensional limit.

To evaluate the chemical potential, the total energy $E(N) = E_{\mathrm{UHFKS}} - \sum_{i=1}^{N}\langle\hat{H}_Z(z_i)\rangle$ is used by subtracting the energy of H_Z from the UHFKS total energy.

The calculated addition energies obtained UHFKS calculation of the single Q-dot are shown in Fig. 1 by comparing with the measured ones [7] depending on the electron number N in Cal.1 and Cal.2 for $\hbar\omega = 5$ meV and 3 meV, respectively.

In these calculations the energy difference between triplet and singlet states of $N = 4$ in $B = 0$ T are about 1.0 meV in both case of $\hbar\omega_0 = 5$ meV and 3 meV but Coulomb energies of the Q-dot of $\hbar\omega_0 = 5$ meV are much

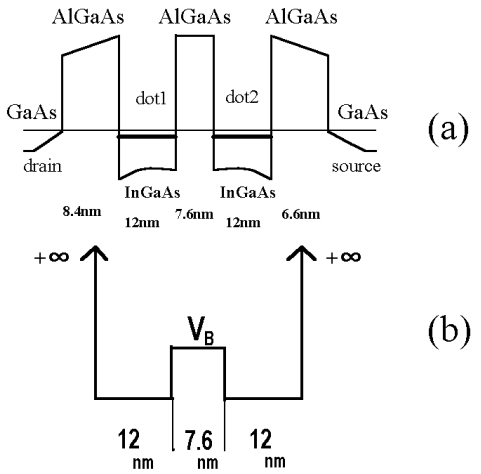

Fig. 3. Schematic presentation of model for coupling between two Q-dots. (a) Experimental profile of TBS [8], (b) model potential $U_Z(z)$ in the vertical direction.

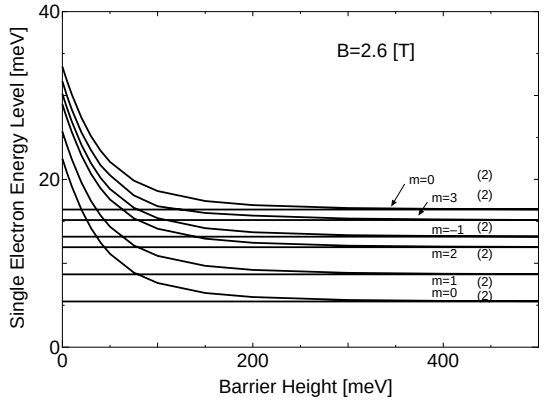

Fig. 4. Barrier height V_B dependence of single electron energies in two quantum dots by 3D-mesh calculation in the case of magnetic field $B = 2.6$ T.

larger than that of $\hbar\omega_0 = 3$ meV which are comparable with measured ones.

To reproduce well the energy difference 0.7 meV between the triplet and singlet states measured in experiment [7], we had to change the dielectric constant as $\epsilon = 25.8$ then the obtained addition energy shown in Fig. 2. In this UHF-calculation we neglected the correlation energy.

4 Coupling between two quantum dots

The $V_Z(z)$ potential which determines the coupling between two Q-dots in TBS is shown in Fig. 3(b) by comparing with experimental profile of Fig. 3(a) [8]. For the 3D-mesh UHF-calculation, the length 31.6 nm of vertical direction as can be seen in Fig. 3(a) is divided into 21 mesh points with equi-distance.

In Fig. 4, the barrier height dependence of single electron energies in two quantum dots by 3D-mesh calculation for the case of $\hbar\omega_0 = 5$ meV and $B = 2.6$ T. Because we

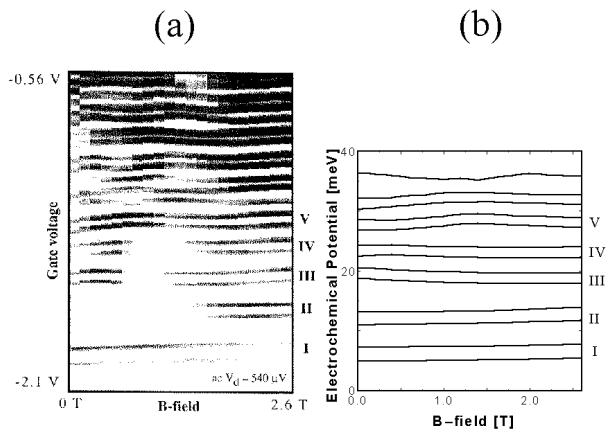

Fig. 5. (a) Magnetic field dependence of measured gate-voltage in TBS [8] and (b) the chemical potential in two quantum dots obtained by 3D-mesh UHF-calculation.

use the symmetrical potential in vertical direction, the very simple bond and anti-bond states are reproduced reasonably well depending on the barrier height V_B in 3D-mesh calculation and the two-body Coulomb energy is more weakened than that of the single Q-dot.

By using the barrier height $V_B = 400$ meV which corresponds weak coupling limit, the chemical potential obtained 3D-mesh UHF-calculation is shown in Fig. 5(b) by comparing the gate voltage shown in Fig. 5(a) of TBS [8]. It is well understood that the magnetic field dependence of the calculated chemical potential well reproduce that of the measured gate voltage in TBS [8] then the spin-degeneracy discussed in [8] appeared in gate-voltage is well reproduced in the small mismatch limit which comes from the doubly degenerated single particle levels shown in Fig. 4.

5 Electronic states in ring structure

Here 3D-mesh UHF-calculation is applied to the calculation of the electronic structure in the ring structure. The confinement potential in xy-plane is used the same one [9] shown in the following $U_C(x, y) = \frac{1}{2}m^*\omega_0^2(r - R_0)^2$ where R_0 is the inner radius of the ring structure. In this calculation, we use the same height 12 nm of the ring structure with the single Q-dot. Because we assume that the ring structure is an ideal symmetric cylinder, we use the $(r, \theta, z)-$cylindrical coordinate for representing the 3D-mesh. The radius coordinate is limited in the region from R_0 to R_{max} and the region is divided in the 20 mesh points with equidistance space. Here we use the $R_{max} = 150$ nm. The angle variable of θ is divided in the equi-angle 20 mesh points from 0 to 2π. By using this 3D-mesh, the calculated single particle of the ring structure is shown in Fig. 6 and obtained almost same magnetic field dependence which is calculated approximately in [9].

Ring size dependence of single particle levels in ring structure by 3D-mesh calculation is shown for the case of $\hbar\omega = 5$ meV from single Q-dot to the larger R_0 as is shown

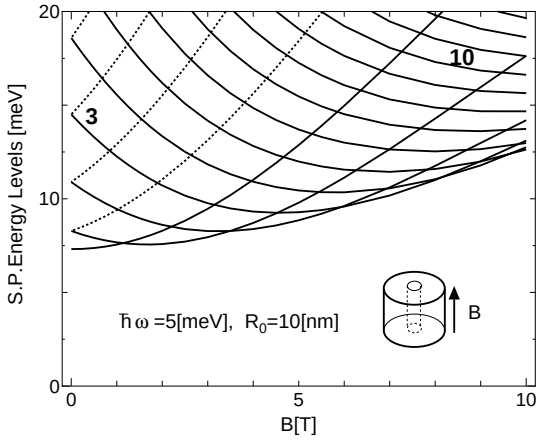

Fig. 6. Magnetic field dependence of single particle levels in ring structure obtained by 3D-mesh calculation.

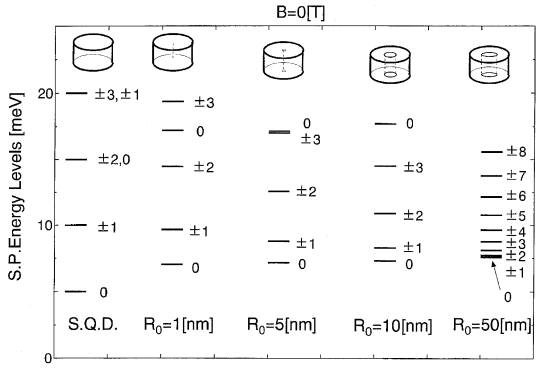

Fig. 7. Ring size dependence of single particle levels in ring structure by 3D-mesh calculation in the case $B = 0$ T.

in Fig. 7. It is very interesting the obtained single particle levels change from vibrational to rotational spectrum by increasing the radius R_0.

In Fig. 8, electron number dependence of addition energy of ring structure $R = 10$ nm obtained by 3D-mesh UHF-calculation for the case of $\hbar\omega = 5$ meV, $\epsilon = 25.8$ and $B = 0$ T.

6 Conclusion

For solving the original nonlinear and nonlocal UHFKS-equation by using 3D-mesh method, the linearization of the equation into the local form has been presented and the 3D-mesh UHFKS-calculation has been applied to the study of the electronic structure of artificial atoms and molecule in created Q-dots.

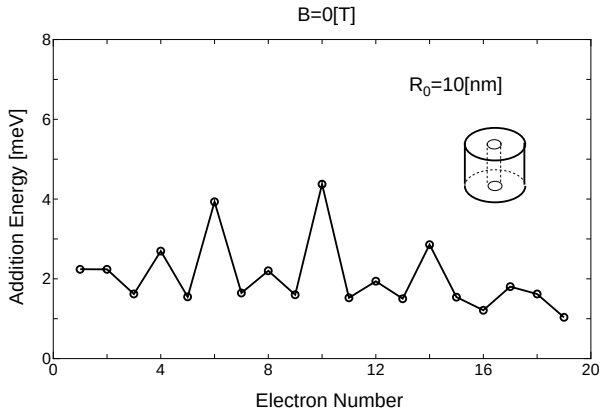

Fig. 8. Electron number dependence of addition energy obtained by 3D-mesh UHF calculation in ring structure of $R_0 = 10$ nm and $B = 0$ T.

Especially it has been shown that the spin-degeneracy measured in gate-voltage depending on magnetic field [8] was shown to be well reproduced in the limit of small mismatch of two Q-dots. Finally, the electronic structures in the ring structure have been calculated and discussed how the ring size and magnetic field affect to the structures without any experimental information.

This work was partly supported by Grant-in-Aid for COE Research (10CE2003) by the Ministry of Education, Science, Sports and Culture of Japan.

References

1. W. Kohn, L.J. Sham, Phys. Rev. **140**, A1133 (1965).
2. J.P. Perdew, A. Zunger, Phys. Rev. B **23**, 5048 (1981).
3. R.G. Parr, W. Yang, *Density-Functional Theory of Atoms and Molecules* (Oxford University Press, 1989).
4. T. Matsuse, *Proceedings of the XVII RCNP International Symposium on "Innovative Computational Methods in Nuclear Many-Body Problems*, edited by H. Horiuchi *et al.* (World Scientific, 1998), p. 369.
5. S.H. Vosko, L. Wilk, J. Phys. B **16**, 3687 (1983).
6. R. Car, M. Parrinello, Phys. Rev. Lett. **25**, 2471 (1985).
7. S. Tarucha, D.G. Austing, T. Honda, R.J. van der Hage, L.P. Kouwenhoven, Phys. Rev. Lett. **77**, 3613 (1996).
8. D.G. Austing, T. Honda, S. Tarucha, Jpn J. Appl. Phys. **36**, 1667 (1997).
9. C.W.J. Beenakker, H. van Houten, A.A.M. Staring, Phys. Rev. B **44**, 1657 (1991).